Int. J. Electrochem. Sci., 14 **(2019)** 3375 – 3392, doi: 10.20964/2019.04.18

International Journal of ELECTROCHEMICAL SCIENCE
www.electrochemsci.org

Electrochemical Studies of the Inhibition Effect of Vitamin B_1 and Bromide Ion on the Carbon Steel Corrosion in Phosphoric Acid Solution

Yan-Ju Yang, Yue-Kun Li, Lin Wang[*]*, Hui Liu, Dong-Mei Lu*[*]*, Li Peng*

School of Chemical Science and Technology, Key Laboratory of Medicinal Chemistry for Nature Resource, Ministry of Education, Yunnan University, Kunming, Yunnan, 650091, P. R. China
[*]E-mail: wanglin@ynu.edu.cn (L. Wang); wanglin2812@163.com

Received: 14 December 2018 / *Accepted:* 14 January 2019 / *Published:* 10 March 2019

This paper investigates the inhibition effects of Vitamin B_1 without and with bromide ion on carbon steel corrosion in 1.0 mol/L phosphoric acid solution using potentiodynamic polarization and electrochemical impedance spectroscopy techniques. The results indicate that combination of Vitamin B_1 and bromide ion performs excellent as inhibitor for carbon steel corrosion in H_3PO_4 solution and a stronger synergistic effect exists between Vitamin B_1 and bromide ion. The electrochemical studies reveal that single Vitamin B_1 acts as a cathodic type inhibitor, but combination of Vitamin B_1 and bromide ion shows as a mixed-type inhibitor and the corrosion reaction is controlled by charge transfer process. Adsorption of VB_1 on the steel surface obeys Langmuir adsorption isotherm in the absence or presence of bromide ion. The thermodynamic and kinetic parameters (ΔG^o_{ads}, ΔH^o_{ads},ΔS^o_{ads}, K_{ads} and E_a) were calculated and discussed. The adsorption of inhibitor molecules on the steel surface is a spontaneous process and chemical adsorption is absolutely dominant.

Keywords: Corrosion inhibition, Vitamin B_1, Carbon steel, Phosphoric acid, Synergistic inhibition.

1. INTRODUCTION

Steel is the most widely used metal material in industrial applications. However, it is often etched during use, especially in acid environment. The application of inhibitors is one of the best ways to inhibit corrosion of metal materials. In view of the need for environmental protection and sustainable development, research on low toxic and non-toxic environment-friendly corrosion inhibitors has gradually attracted attention [1-4]. The several non-toxic rare earth carboxylate compounds have been synthesized and studied as corrosion inhibitors for mild steel [5-6]. Some of low toxic surfactants have also been used as corrosion inhibitors and shown high inhibition efficiencies for

steel in acidic solution [7-8]. Plant extracts have become important sources of corrosion inhibitor because they are low cost, readily available and eco-friendly [9], such as Gum Arabic [10], Cucumis Saativus peel [11], Coffee Ground [12], Garlic peel [13], Watermelon Rind[14]. Some medicines are also environmentally friendly and can be used as green corrosion inhibitors [1,15]. Cefatrexyl shows excellent inhibition performance on iron corrosion in H_2SO_4, $HClO_4$ and H_3PO_4 [16]. Ampicillin and halide ions (Cl^-, Br^-, I^-) have good synergistic effect for mild steel corrosion inhibition in H_2SO_4 [17]. Streptomycin acted as a good inhibitor for the corrosion of mild steel in HCl solution [18]. Salbutamolcan effectively inhibit corrosion of low carbon steel in HCl solution and exhibit strong chemical adsorption on steel surface [19]. Vitamins have a good promoting effect on human health and are also used as corrosion inhibitors. Fuchs- Godec et al studied the inhibition abilities of vitamin C on the steel corrosion in HCl and results shown that vitamin C is a mixed- type inhibitor and a good inhibition efficiency [20]. Fuchs- Godec et al also studied the modification of Cu and Cu40Zn surfaces by stearic acid and vitamin E, which indicated that vitamin E additional effectively improved the inhibitory properties [21]. Some studies show that vitamins B and their derivatives have better corrosion inhibitions for various metals in different media [22-23]. Bhola et al investigated that inhibition of nickle corrosion by vitamin B_1 in HNO_3 solution and found it is a good inhibitor [24]. Hoseinzadeh et al reported that vitamin B_1 retards both anodic and cathodic reactions by blocking the active corrosion sites for AISI steel 4130 in HCl solution [25]. Qiao's study indicated that the combination of Lysozyme and vitamin B_1 is more effective inhibitor for carbon steel corrosion in H_2SO_4 solution [26]. Solmaz found that vitamin B_1 acts by adsorption on the mild steel through chemical and physical interactions and form a very stable protective film on the surface in HCl solution [27].

This work attempts to exhibit the kinetic parameters of carbon steel corrosion and the synergistic inhibition effect and the adsorption thermodynamic parameters of vitamin B_1 and bromide ion inhibitors on carbon steel in 1.0 ml/L H_3PO_4 by the measurements of potentiodynamic polarization and electrochemical impedance spectroscopy (EIS).

2. EXPERIMENTAL

2.1. Materials

The carbon steel specimens have a chemical composition of (wt%): 0.15% C, 0.020% S, 0.029% P, 0.058% Si, 0.34% Mn and Fe balance.

Theexperimental solutions were prepared using bidistilled water and AR grade H_3PO_4 and potassium bromide (KBr) were used too. Vitamin B_1 (VB_1) was supplied by Merck Chemicals. Figure 1 gives the chemical structure of VB_1.

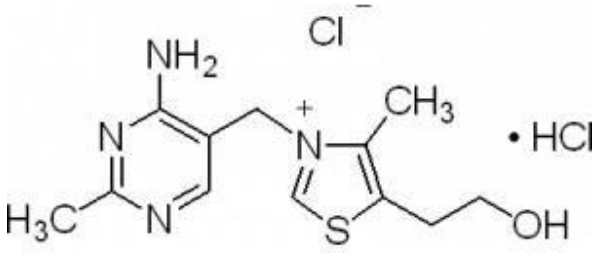

Figure 1. Structure of VB_1.

2.2. Electrochemical measurements

An electrochemical cell with a conventional three-electrode was applied to electrochemical measurements. The reference electrode was saturated calomel electrode (SCE) and auxiliary electrode was a platinum foil.The working electrodes were embedded in PVC holder using epoxy resin with an exposed area of 1.0 cm^2. Each working electrode was polished using emery papers (300 - 1200 grade) on the test face, washed with distilled water, degreased with acetone, and dried with a warm air stream. Before each measurement, the working electrode was immersed for two hours in the 250 ml testing solution at open circuit potential until corrosion potential reached a steady state.

All the electrochemical experiments were performed using PARSTAT 2263 Potentiostat/Galvanostat (Princeton Applied Research). The Tafel polarization curves were obtained by changing the electrode potential from -250mV to + 250mV versus the open circuit potential, at a scanning rate of 0.5 mVs^{-1}. EIS experiments were performed in the frequency range of 100 kHz to 10 mHz using a 10 mV peak to peak voltage excitation. Each experiment was performed in triplicate to ensure reproducibility.

3. RESULTS AND DISCUSSION

3.1. Polarization measurements

Figure 2 gives the potentiodynamic polarization curves of carbon steel in 1.0mol/L H_3PO_4 at 25 ℃ for different concentrations of VB_1 without and with 50 mmol/L Br^-.

By Figure 2 (a), the corrosion potentials do not change remarkably and anodic current densities show a slight increase or decrease compared with the blank with the increase of VB_1 concentrations, but cathodic polarization is obvious and the current densities decreases as increasing VB_1 concentrations. These mean that VB_1 could retard the hydrogen evolution reaction as a cathodic inhibitor. From Figure 2 (b), the shifts of anodic and cathodic branches are clear and cathodic polarization is obviously dominant with addition of 50 mmol/L Br^-, which indicates that the combination of VB_1 and Br^- is a mixed-type inhibitor for carbon steel corrosion in H_3PO_4.

The inhibition efficiency (*IE*) is calculated by the formula [28]:

$$IE = \frac{i_{coor}^{0} - i_{coor}^{inh}}{i_{coor}^{0}} \times 100 \qquad (1)$$

where i_{corr}^{0} and i_{corr}^{inh} are the corrosion current density values without and with inhibitors, respectively.

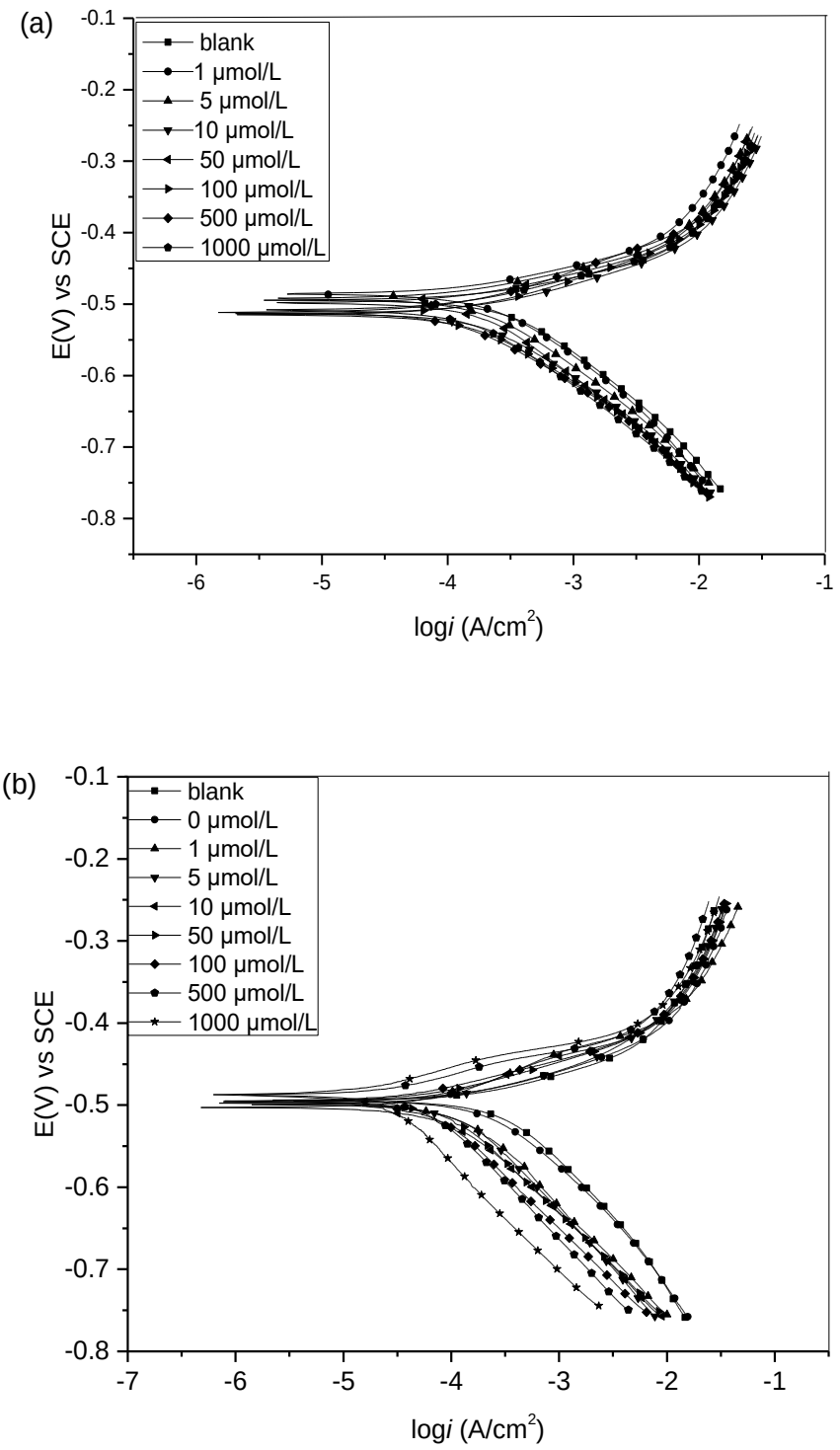

Figure 2. The potentiodynamic polarization curves of carbon steel in 1.0 mol/L H_3PO_4 at 25℃ for different concentrations of VB_1 in the absence (a) and presence (b) of 50 mmol/L Br^-.

Table 1 illustrates corrosion potential (E_{corr}), anodic and cathodic Tafel slopes (β_a, β_c), corrosion current density (i_{corr}) and the inhibition efficiencies for the carbon steel corrosion by VB_1 in the absence and presence Br^- in 1.0 mol/L H_3PO_4. As seen, Tafel slopes of β_a and β_c do not change remarkably with the addition of VB_1 or VB_1 and Br^-, meaning that the presence of VB_1 or VB_1 and Br^- does not change the reaction mechanism of carbon steel corrosion in 1.0 mol/L H_3PO_4 at 25 ℃. Comparing with the inhibition efficiencies, the *IE*s of combination of VB_1 and Br^- are much greater than those of single VB_1 and the highest *IE* is up to 90% at 1000 μmol/L VB_1 and 50 mmol/L Br^-. The change of E_{corr} is slight in the presence of the inhibitor, therefore, the inhibition of VB_1 and Br^- on carbon steel is caused by geometric blocking effect coming from the reduction of the reaction area on the surface of the corroding metal [29].

Table 1. Polarization parameters for carbon steel corrosion containing inhibitors in 1.0 mol/L H_3PO_4 at 25 ℃.

VB_1 （μmol/L）	Br^- (mmol/L)	E_{corr} (vs SCE) (mv)	i_{corr} ($\mu A/cm^2$)	β_a (mV/dec)	$-\beta_c$ (mV/dec)	IE (%)
0	0	-494	374	93	153	-
1	0	-486	352	96	172	6
5	0	-513	310	90	157	17
10	0	-492	281	89	158	25
50	0	-503	267	77	159	29
100	0	-515	257	91	151	31
500	0	-512	223	104	147	40
1000	0	-508	205	74	149	45
0	50	-494	271	63	142	28
1	50	-498	156	81	148	58
5	50	-499	131	52	146	65
10	50	-495	98.0	59	137	74
50	50	-496	96.3	86	152	74
100	50	-503	82.9	54	123	78
500	50	-493	60.4	51	140	84
1000	50	-488	35.7	75	154	90

The changes of the carbon steel corrosion at different concentration of VB_1 with the temperature were also researched without and with 50 mmol/L Br^-. The polarization curves at 30, 40 ℃ were given in Figure 3 and Figure 4, respectively. The corresponding potentiodynamic polarization parameters are illustrated in Table 2, Table 3 too.

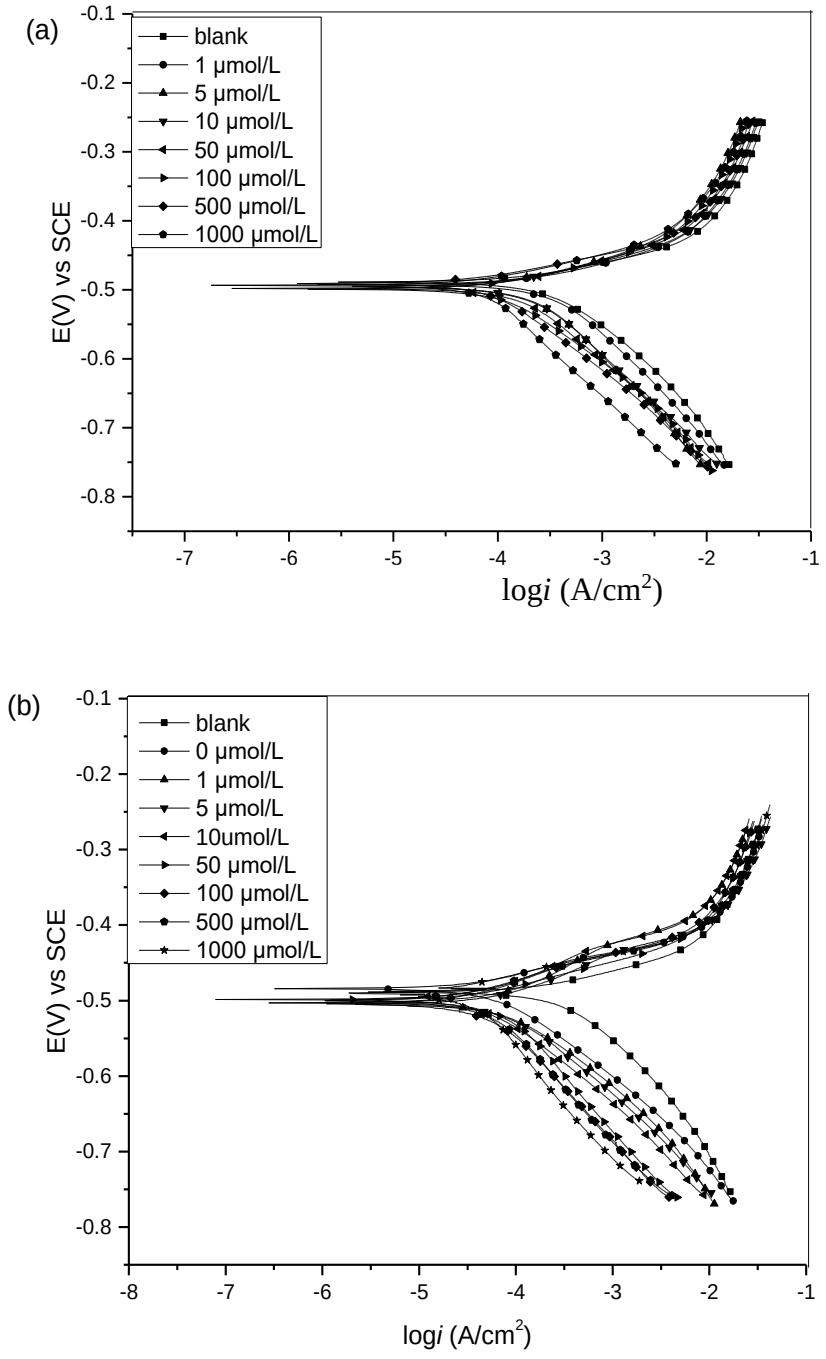

Figure 3. The potentiodynamic polarization curves of carbon steel in 1.0 mol/L H_3PO_4 at 30℃ for different concentrations of VB_1 in the absence (a) and presence (b) of 50 mmol/L Br^-.

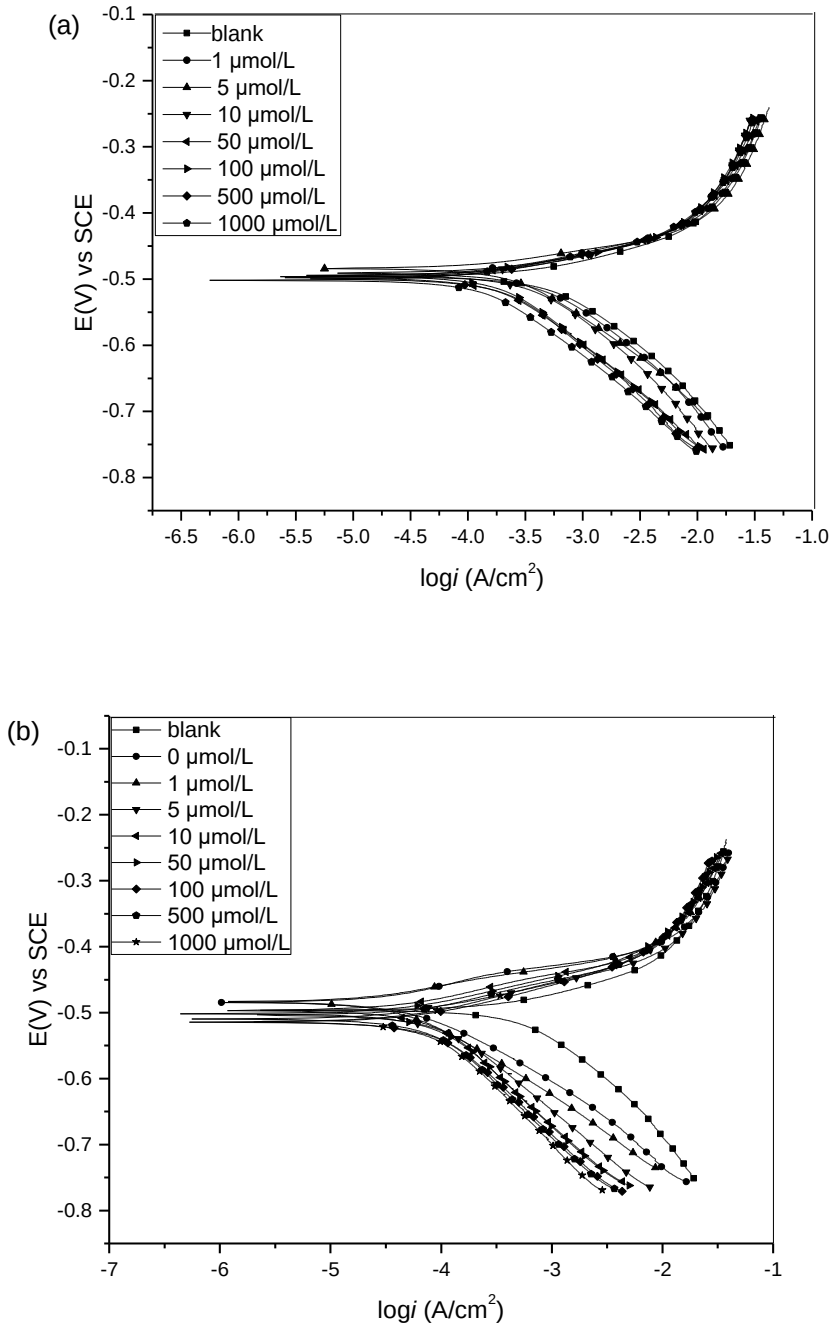

Figure 4. The potentiodynamic polarization curves of carbon steel in 1.0 mol/L H_3PO_4 at 40℃ for different concentrations of VB_1 in the absence (a) and presence (b) of 50 mmol/L Br^-.

It can be seen that raising the temperature has no significant effect on the corrosion potentials and Tafel slopes of β_a and β_c. The corrosion current densities basically show a slight downward trend by increasing in temperature in the combination of VB_1 and Br^-. For single VB_1, the current densities fluctuate slightly with increasing temperature, but there is still a slight increase of current densities with the increase of the temperature in the whole.

Table 2. Polarization parameters for carbon steel corrosion containing inhibitors in 1.0 mol/L H_3PO_4 at 30 ℃.

VB_1 （μmol/L）	Br^- (mmol/L)	E_{corr} (vs SCE) (mv)	i_{corr} (μA/cm^2)	β_a (mV/dec)	$-\beta_c$ (mV/dec)	IE (%)
0	0	-489	420	64	155	-
1	0	-482	378	63	158	10
5	0	-496	307	87	180	27
10	0	-495	295	83	165	30
50	0	-498	194	86	164	54
100	0	-499	176	107	157	58
500	0	-491	161	92	146	62
1000	0	-494	122	87	176	71
0	50	-507	259	86	163	38
1	50	-497	137	83	121	67
5	50	-503	125	82	124	70
10	50	-484	100	68	121	76
50	50	-505	90.0	61	118	79
100	50	-499	71.5	77	123	83
500	50	-500	48.4	53	141	88
1000	50	-489	29.5	35	143	93

Table 3. Polarization parameters for carbon steel corrosion containing inhibitors in 1.0 mol/L H_3PO_4 at 40 ℃.

VB_1 （μmol/L）	Br^- (mmol/L)	E_{corr} (vs SCE) (mv)	i_{corr} (μA/cm^2)	β_a (mV/dec)	$-\beta_c$ (mV/dec)	IE (%)
0	0	-496	689	74	163	-
1	0	-491	550	81	162	20
5	0	-494	479	76	175	30
10	0	-484	365	69	149	47
50	0	-500	287	71	174	58
100	0	-495	260	67	167	62
500	0	-498	238	66	155	65
1000	0	-502	191	69	154.	72
0	50	-510	359	79	148	48
1	50	-502	199	87	177	71
5	50	-515	110	86	130	84
10	50	-502	103	86	137	85

50	50	-503	64.8	78	142	91
100	50	-498	59.2	53	108	91
500	50	-496	41.9	45	179	94
1000	50	-502	28.0	48	142	96

It is also obvious that the values of *IE* increase gradually by increasing temperature at same concentration of VB_1 in the absence and presence of Br^-. Increasing temperature is beneficial to the protection of the inhibitors for carbon steel and the combination of VB_1 and Br^- still can show more effective inhibition than single VB_1 at experimental temperatures.

3.2. Adsorption isotherm

Adsorption isotherms could be commonly used to know the some information on the interaction between inhibitor and steel surface. The Langmuir adsorption isotherm was used to understand the adsorption mechanism as follow [30]:

$$\frac{C}{\theta} = \frac{1}{K_{ads}} + C \qquad (2)$$

where C is the concentration of the inhibitor, θ is the surface coverage of inhibitor molecules and Kads is the adsorptive equilibrium constant.

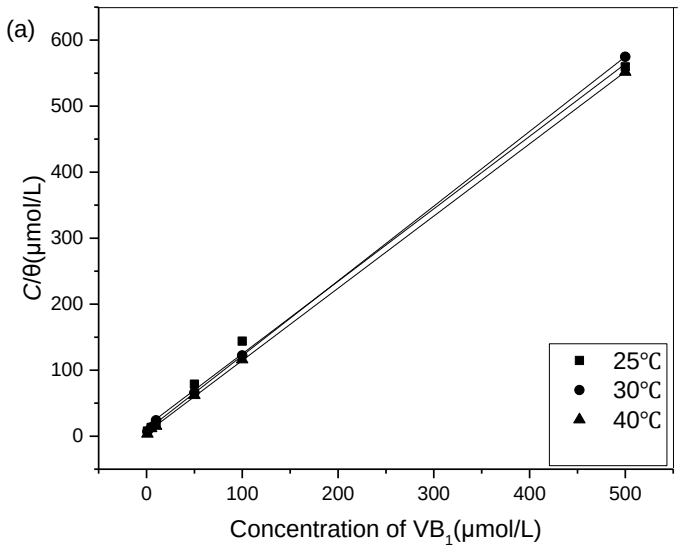

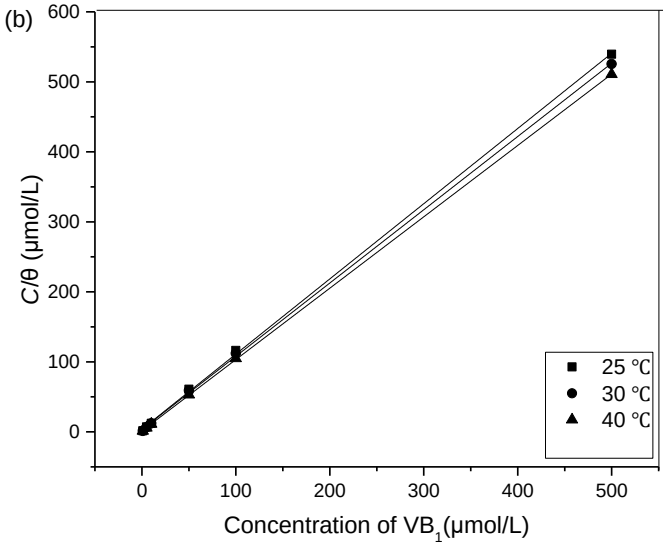

Figure 5. The relationship between C/θ and C in the absence (a) and presence (b) of Br^-.

The surface coverage (θ) was calculated by using the equation:

$$\theta = \frac{i_{corr}^{0} - i_{corr}^{inh}}{i_{corr}^{0} - i_{m}^{inh}} \qquad (3)$$

where i_m^{inh} is the smallest corrosion current density.

The relationship between C/θ and C in the absence (a) and presence (b) of Br^- is shown in Figure 5 and the corresponding parameters obtained are also listed in Table 4.

Table 4. Parameters of the linear regression between C/θ and C .

Inhibitor	Temperature （℃）	Linear regression coefficient	K_{ads} ($\times 10^4$ L/mol)
VB_1	25	0.9971	6.66
VB_1	30	0.9999	11.3
VB_1	40	0.9999	18.7
$VB_1 + Br^-$	25	0.9997	27.3
$VB_1 + Br^-$	30	0.9997	30.1
$VB_1 + Br^-$	40	1.0000	75.9

It is clear that the linear regression coefficient values are very close to unity, meaning that the adsorption of VB_1 on the carbon steel surface obeys the Langmuir adsorption isotherm without or with Br^-. it can also be seen that the values of K_{ads} are large to 10^4, showing there is strong adsorption VB_1 onto the steel surface. Compared the values of K_{ads} in the absence and presence of Br^-, it is found that the values of K_{ads} are larger with Br^- than the without, which indicates the trend of adsorption of combination of VB_1 and Br^- is stronger than single presence of VB_1.

From the thermodynamic model, the adsorption phenomenon of inhibitor and the corrosion inhibition of carbon steel can be better explained using some thermodynamic parameters. According to the Van't Hoff equation [31]:

$$\ln K_{ads} = \frac{-\Delta H^{\circ}_{ads}}{RT} + B \qquad (4)$$

where ΔH^{o}_{ads} is the standard adsorption heat. T is the absolute temperature, B is a constant. Clearly, from the slope of the regression the adsorption heat can be calculated.

The standard adsorption free energy (ΔG^{o}_{ads}) can also be obtained by the following calculation [32-33]:

$$K_{ads} = \frac{1}{55.5}\exp(\frac{-\Delta G^{\circ}_{ads}}{RT}) \qquad (5)$$

where the value 55.5 is the concentration of water in solution represented in mol/L. The standard adsorption entropy (ΔS^{o}_{ads}) can be calculated by the basic thermodynamic equation:

$$\Delta G^{o}_{ads} = \Delta H^{o}_{ads} - T\Delta S^{o}_{ads} \qquad (6)$$

The thermodynamic parameters calculated are listed in Table 5.

Table 5. The thermodynamic parameters of adsorption of VB_1 or VB_1 + Br^- on the carbon steel surface in 1.0 mol/L H_3PO_4 at different temperatures.

Inhibitor	Temperature (℃)	ΔG^{o}_{ads} (kJ/mol)	ΔH^{o}_{ads} (kJ/mol)	ΔS^{o}_{ads} (J/mol K)
VB_1	25	-37	51	297
VB_1	30	-39	51	299
VB_1	40	-42	51	298
VB_1 + Br^-	25	-41	56	325
VB_1 + Br^-	30	-42	56	323
VB_1 + Br^-	40	-46	56	325

From Table 5, the positive values of ΔH^{o}_{ads} mean that the adsorption of the VB_1 on the carbon steel surface is an endothermic process in the absence or presence of Br^- in 1.0 mol/L H_3PO_4.

It is known that the values of ΔG^{o}_{ads} around -20 kJ/mol or less negative are assigned for the electrostatic interactions exist between inhibitor and the charged metal surface (physisorption). While those around -40 kJ/mol or more negative are associated with chemisorption as a result of sharing or transferring of electrons from the inhibitor molecules to the metal surface to form a coordinate type of metal bond [34-35].

Whether bromine ion exists or not in 1.0 mol/L H_3PO_4 solution, the negative values of ΔG^{o}_{ads} show spontaneous adsorption process of VB_1 on the carbon steel surface. These values of ΔG^{o}_{ads} suggest that adsorption mechanism of the inhibitor molecules on the carbon steel is mainly chemisorption, especially when VB_1 and Br^- coexist, it is completely chemical adsorption. The

increase of free energy and inhibition efficiency with the increase of temperature indicates that the adsorption of the inhibitor on the carbon steel is beneficial at higher temperature in H_3PO_4 solution.

The positive values of ΔS^{o}_{ads} shows that the adsorption is a process of entropy increase and the increase of entropy is the driving force of spontaneous process inhibitor molecules adsorbed on the surface of carbon steel. The entropy increases can be attributed to the increase in the solvent entropy because more water molecules are replaced by one inhibitor molecule and desorbed from the metal surface [36-37].

3.3. Effect of temperature

The mechanism of the inhibitors action can be further elucidated by kinetic model and Arrenius formula was applied to calculate the activation parameters:

$$\ln i_{corr} = \frac{-E_a}{RT} + \ln A \qquad (7)$$

where E_a is apparent activation energy and A is pre-exponential factor. The plots of ln i_{corr} vs. 1/T is given in Figure 6.

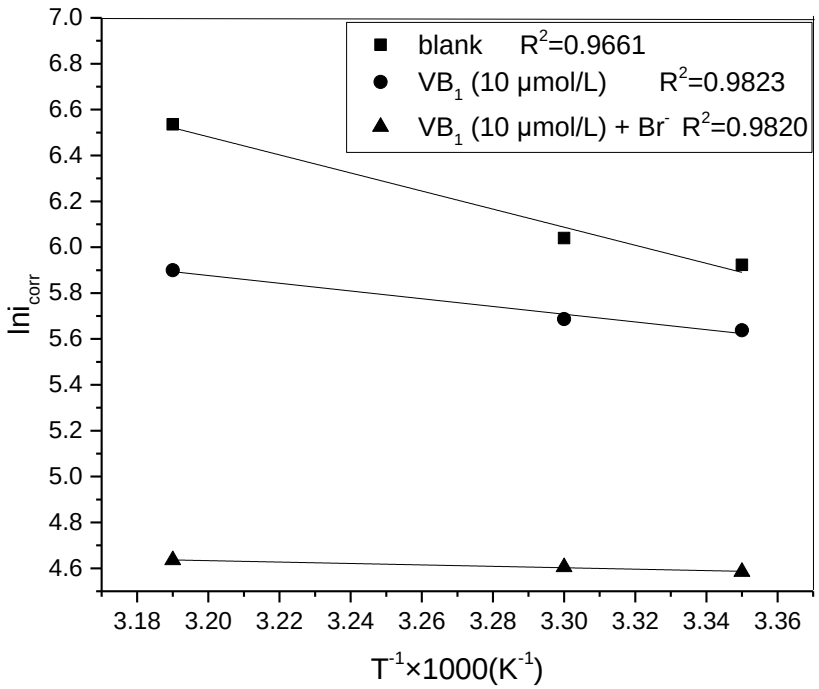

Figure 6. Arrhenius plots of carbon steel without and with VB_1 or VB_1 + Br^- in 1.0 mol/L H_3PO_4.

From the Arrhenius plots, the apparent activation energies of the corrosion process were calculated as 33 kJ/mol for the blank, 14 kJ/mol for VB_1 and 3 kJ/mol for VB_1 + Br^-. It can be found that the addition of VB_1 or VB_1 + Br^- to H_3PO_4 solution decreases the E_a, meaning that it is easier for

VB_1 or VB_1 + Br^- to be adsorbed on carbon steel surface and corrosion rate even decrease at higher temperature. The reduction of the activation energies with the addition of inhibitor is indicative of chemisorption of the inhibitor molecules on the metal surface [38-39], which is consistent with the result of adsorption free energy.

3.4. Electrochemical impedance spectroscopy

Nyquist plots for carbon steel at 40 ℃ are presented in Figure 7.

It is obvious that only a single capacitive loop depressed semicircles is observed for all the Nyquist impedance plots, which suggests that the corrosion process occurs under charge transfer control. The inhibition of steel corrosion was influenced predominantly by charge-transfer process and the existence of inhibitors did not affect the mechanism of steel dissolution [40]. The capacitive loops are imperfect semicircles which can be attributed to the frequency dispersion effect as a result of the roughness and inhomogeneous of the electrode surface [41]. It is also found that diameters of the capacitance loops are clearly bigger in the presence of Br^- than in the absence of Br^-, revealing that the presence of Br^- can improve corrosion performance of VB_1 effectively.

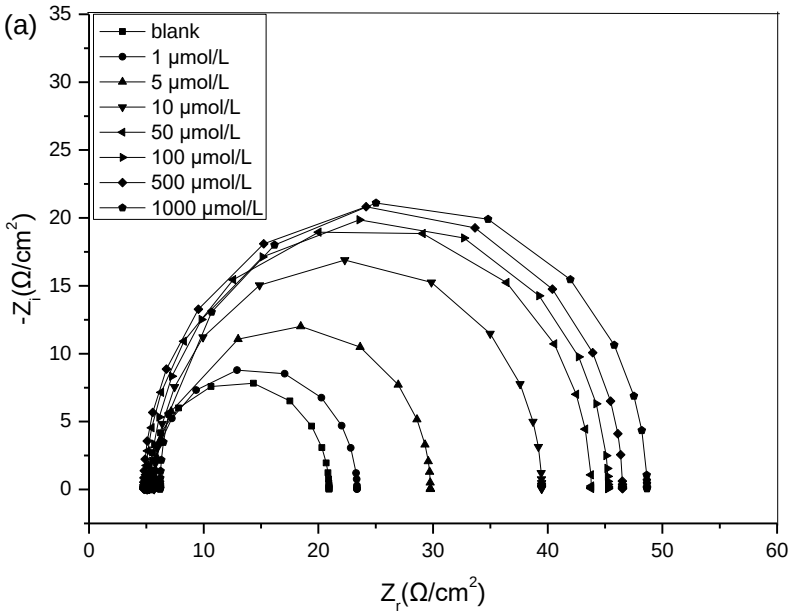

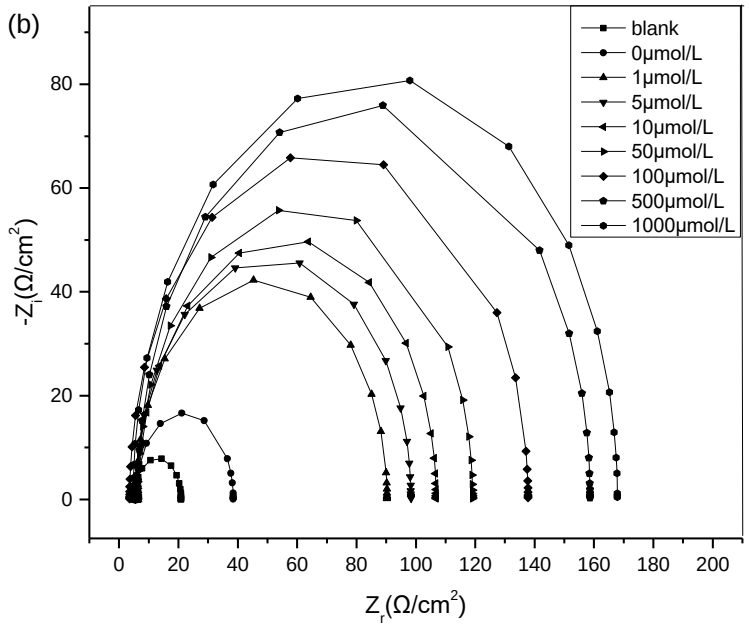

Figure 7. The Nyquist plots for carbon steel in 1.0 mol/L H_3PO_4 at 40°C for different concentrations of VB_1 in the absence (a) and presence (b) of 50 mmol/L Br^-.

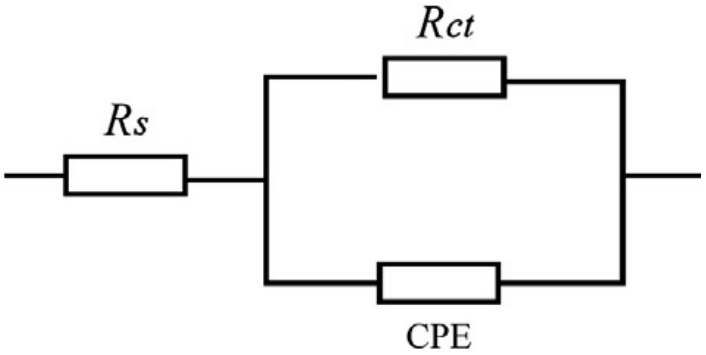

Figure 8. Equivalent circuit used to fit the capacitive loop.

The electrochemical impedance spectroscopy results are simulated according to the equivalent circuit model which is well-known Randle cell, shown in Figure 8, which includes charge transfer resistance (R_{ct}), solution resistance (R_s) and a constant phase element (CPE). The double layer capacitance (C_{dl}) value affected by imperfections of the surface is simulated via CPE [42]. The CPE is composed of a component Q_{dl} and a coefficient α which quantifies different physical phenomena including surface inhomogeneous resulting from surface roughness, porous layer formation, inhibitor adsorption, etc. The C_{dl} can be obtained as follows [43]:

$$C_{dl} = Q_{dl} \cdot (2\pi f_{max})^{\alpha-1} \quad (8)$$

where f_{max} represents the frequency at which the imaginary value reaches a maximum on the Nyquist plot.

The inhibition efficiencies were calculated as follow:

$$IE_t = \frac{R_{ct(inh)} - R_{ct(0)}}{R_{ct(inh)}} \times 100 \qquad (9)$$

where $R_{ct(0)}$ and $R_{ct(inh)}$ are the charge-transfer resistances in the absence and presence of inhibitor, respectively. The values of EIS parameters are illustrated in Table 6.

Table 6. EIS parameters for carbon steel corrosion containing inhibitors in 1.0 mol/L H_3PO_4 at 40 ℃.

VB_1 （μmol/L）	Br^- (mmol/L)	R_s (Ω cm^2)	C_{dl} (μF/cm^2)	R_{ct} (Ω cm^2)	IE_{ct} (%)
0	0	5.06	173	15.9	-
1	0	5.52	135	17.8	11
5	0	5.69	78.9	24.1	34
10	0	5.68	60.7	33.8	53
50	0	4.92	65.2	38.9	59
100	0	4.82	55.1	39.9	60
500	0	4.77	52.0	41.8	62
1000	0	6.20	53.3	42.5	63
0	50	5.42	63.4	33.3	52
1	50	4.76	47.0	54.5	71
5	50	5.64	40.9	84.7	81
10	50	6.52	28.1	100	84
50	50	6.23	21.0	113	86
100	50	3.59	18.3	134	88
500	50	6.30	19.6	152	90
1000	50	4.74	17.3	163	90

Compared with the blank solution, the capacitance values decrease in the presence of the inhibitor and they show a gradual downward trend with the increase of VB_1 concentration, which means that the decrease of C_{dl} is resulted from the decrease in local dielectric constant or the increase in the thickness of the electrical double layer, suggesting the adsorption of inhibitor molecules at the metal/solution interface [44]. At the same time, It can be observed that R_{ct} and IE_{ct} also increase with the increase of VB_1 concentration, regardless of whether Br^- exists or not. Of course, this is also obvious that the R_{ct} or IE_{ct} in the presence of Br^- are much larger than those in the absence of Br^-. These results are in good agreement with those obtained from polarization measurements.

3.7. Synergism parameters

From the above studies, it is found that the inhibition efficiency for solution with Br^- exhibit greater values compared to solution without Br^-. That is to say, the addition of 50 mmol/L Br^- effectively improves the increase of inhibition efficiency comparing with single VB_1. This reflects that

there may be a synergistic inhibition effect of VB_1 and Br^- for carbon steel corrosion in 1.0 mol/L H_3PO_4, which can be examined using synergism parameters (S), defined as follows [45]:

$$S = \frac{1 - IE_1 - IE_2 + IE_1 IE_2}{1 - IE_{1+2}} \qquad (10)$$

where IE_1 and IE_2 are the inhibition efficiencies by inhibitor 1 or by inhibitor 2, respectively, and IE_{1+2} is the inhibition efficiency by both inhibitor 1 and inhibitor 2.

Generally, when value of S is < 1, implying that antagonistic behavior leading to competitive adsorption prevails, whereas S > 1 means a synergistic effect. Table 8 gives the values of S. It is obvious that all S values are greater than 1 and behave larger, indicating that VB_1 and Br^- have stronger synergistic inhibition effect on carbon steel corrosion and promote the inhibition efficiency to be greatly improved in 1.0 mol/L H_3PO_4.

Table 7. Synergism parameters of VB_1 and Br^- on the corrosion inhibition of carbon steel in 1.0 mol/L H_3PO_4 at experimental temperatures.

VB_1 (μmol/L)	Br^- (mmol/L)	Synergism parameters(S)		
		25℃	30℃	40℃
1	50	1.61	1.69	1.43
5	50	1.71	1.51	2.28
10	50	2.08	1.81	1.84
50	50	1.97	1.36	2.43
100	50	2.15	1.53	2.20
500	50	2.70	1.96	3.03
1000	50	3.96	2.57	3.64

In acid solution, steel surface contains positive charge due to $E_{corr} - E_{q=0}$ (zero charge potential) > 0 [46], and VB_1 can also be protonated into $[VB_1H_x]^{x+}$. Therefore, the adsorption of corrosion inhibitor on steel is first shown as electrostatic action. Due to electrostatic repulsion, it is difficult for positive charged VB_1 to approach the positive charged position on the surface of steel. On the contrary, negatively charged Br^- is easily adsorbed to the positively charged position of steel surface, resulting in potential of zero charge becomes less negative which promotes the adsorption of inhibitors in cationic form [47]. The adsorption of VB_1 molecules can occur through donor-acceptor interactions between the nitrogen, sulfur atoms or abundance π-electrons of VB_1 and the unoccupied d-orbital of the iron atoms [48]. Thus, it is shown as chemical adsorption. So, physical and chemical adsorption may be acting on the carbon steel surface.

4. CONCLUSION

The corrosion of the carbon steel in 1.0 mol/L H_3PO_4 is not significantly reduced upon the addition of single VB_1 or Br^-. However, the inhibition efficiency of combination of VB_1 and Br^- is

enormously improved. The synergism parameters reveal that a stronger synergistic inhibition effect exists between VB_1 and Br^- for carbon steel corrosion in H_3PO_4. The adsorption of VB_1 on the steel surface follows the Langmuir adsorption isotherm in the absence or presence of Br^-. The adsorption of inhibitor molecules on the steel surface is a spontaneous process and chemical adsorption is absolutely dominant.

Single VB_1 acts as a cathodic type inhibitor, but combination of VB_1 and Br^- acts as a mixed-type inhibitor for carbon steel corrosion in 1.0 mol/L H_3PO_4. EIS shows that the fact the corrosion reaction is controlled by charge transfer.

ACKNOWLEDGEMENT:
This work was financially supported by the National Innovation and Entrepreneurship of College Students Foundation of China (Grant No.201610673001).

References

1. G. Gece, *Corros. Sci.,* 53 (2011) 3873.
2. K.W. Tan and M.J. Kassim, *Sci.,* 53 (2011) 569.
3. M.A. Quraishi, A. Singh, V.K. Singh, D.K. Yadav and A.S. Singh, *Mater. Chem. Phys*., 122 (2010) 114.
4. Y. Hao, L.A. Sani, T, Ge and Q. Fang, *Sci.,* 123 (2017) 158.
5. C.N. de Bruin-Dickason, G.B. Deacon, C.M. Forsyth, S. Hanf, O.B. Heilmann, B.R.W. Hinton, P.C. Junk, A.E. Somers, Y.Q. Tan and D.R. Terner, *Aust. J. Chem.*, 70 (2017) 478.
6. A.E. Somers, B.R.W. Hinton, C. de Bruin-Dickason, G.B. Deacon, P.C. Junk and M. Forsyth, *Corros. Sci.,* 139 (2018) 430.
7. G. Banerjee and S.N. Malhorta, *Corrosion*, 48 (1992) 10.
8. B.A. Abd-El-Naby, O.A. Abdullatef, E. Khamis and W.A. El-Mahmody, *Int. J. Electrochem. Sci*., 11 (2016) 1271.
9. M. Majeed, A. Sultan and H. Al-Sahlanee, *J. Chem. Pharma. Res*., 5 (2013) 1297.
10. K. Azzaoui, E. Mejdoubi, S. Jodeh, A. Lamhamdi, E. Rodriguez-Castellon, M. Algarra, A. Zarrouk, A. Errich, R. Salghi and H. Lgaz, *Corros. Sci.,* 129 (2017) 70.
11. G.M. Al-Senani, *Int. J. Electrochem. Sci*., 11 (2016) 291.
12. V.V. Torres, R.S. Amado, C.F. de Sa, T.L. Fernandez, C. A. da Silva Riehl, A. G. Torres and E. D'Elia, *Corros. Sci.,* 53 (2011) 2385.
13. S.S. de Assunção Araujo Pereira, M.M. Pêgas, T.L.Fernández, M. Magalhaes, T.G. Schöntag, D.C. Lago, L.F. de Senna and E. D'Elia, *Corros. Sci.,* 65 (2012) 360.
14. N. Odewunmi, S. Umoren and Z. Gasem, *J. Ind. Eng. Chem.*,21 (2015) 239.
15. C. Verma, D.S. Chauhan and M.A. Quraishi, *J. Mater. Environ. Sci.*, 8 (2017) 4040.
16. M.S. Morad, *Corros. Sci.,* 50 (2008) 436.
17. N.O. Eddy, E.E. Ebenso and U.J. Ibok, *J. Appl. Electrochem*., 40 (2010) 445.
18. S.K. Shukla, E.E Ebenso, *Int. J. Electrochem. Sci*., 6 (2011) 3277.
19. P. Geethamani, P.K. Kasthurl and S. Aejitha, *Int. J. Chem. Pharma. Sci*. 3 (2015) 1442.
20. R. Fuchs-Godec, M.G. Povlovic and M.V. Tomic, *Int. J. Electrochem. Sci*., 8 (2013) 1511.
21. R. Fuchs-Godec and G. Zerjav, *Corros. Sci.,* 97 (2015) 7.
22. H. Ju, Q. Li and Y. Ju, *Adv. Mater. Res*., 562-584 (2012) 184.
23. O.K. Abiola, *Corros. Sci.,*48 (2006) 3078.
24. S.M. Bhola, C. Chandra and G. Singh, *J. Corros. Sci. Eng.,* 11 (2008) 1.

25. A.R. Hoseinzadeh, I. Danaee and M.H. Maddahy, *Z. Phys. Chem*., 227 (2013) 403.
26. K. Qiao, Y. Wu and X. Liu.*Adv. Mater. Res*., 463-464 (2012) 895.
27. R. Solmaz, *Corros. Sci.,* 81 (2014) 75.
28. M. Shahin, S. Bilgie and H Yilnaz, *Appli. Surf. Sci*., 195 (2002) 1.
29. C Cao, *Corros. Sci.*, 38 (1996) 2073.
30. E.A. Noor and A.H. Al-Moubaraki, *Mater. Chem. Phys.*, 110 (2008) 145.
31. L. Wang, H. Zheng, X.M. Zi, S.W. Zhang, L. Peng and J. Xiong, *Int. J. Electrochem. Sci*., 11 (2016) 6609.
32. M. Lebrini, M. Lagrenée, H.Vezin, M. Traisnel and F. Bentiss, *Corros. Sci*,. 49 (2007) 2254.
33. S.K. Shukla and M.A. Quraishi, *Corros. Sci.*, 51 (2009) 1007.
34. E. Machnikova, K. H. Whitmire and N. Hackerman, *Electrochim. Acta*, 53 (2008) 6024.
35. R. Fuchs-Godec and V. DlecekA, *Collodis Surf.* A., 244 (2004) 73.
36. R. Solmaz, G. Kardaş, M. Çulha, B. Yazici and M. Erbil, *Electrochim. Acta*, 53 (2008) 5941.
37. G. Avci, *Colloid Surf. A*, 317 (2008) 730.
38. T. Szauer and A. Brandt, *Electrochim. Acta*, 26 (1981) 193.
39. N. Soltani, M. Behpourb, S.M. Ghoreishi and H. Naeimi, *Corros. Sci.*, 52 (2010) 1351.
40. L. Larabi, Y. Harek, M. Traisnel and A.Mansri, *J. Appl. Electrochem.,* 34 (2004) 833.
41. M. Lebrini, M. Lagrenée, M. Traisnel, L. Genembre, H. Vezin and F. Bentiss,*Appl. Surf. Sci.*, 253 (2007) 9267.
42. P. Bommersbach, C. Alemany-Dumont, J.P. Millet and B. Normand, *Electrochim. Acta,* 51 (2006) 4011.
43. M. Lagrenėe, B. Mernari, M. Bouanis, M. Traisnel and F. Bentiss, *Corros. Sci.*, 44 (2002) 573.
44. M. Behpour, S.M. Ghoreishi, M. Khayatkashani and N. Soltani, *Corros. Sci.,* 53 (2011) 2489.
45. T. Murakawa,S. Nagaura and N. Hackerman, *Corros. Sci*., 7 (1967) 79.
46. A. Döner, E.A. Şuhin, G. Kardaş and O. Serindağ, *Corros. Sci.*, 66 (2013) 278.
47. H. Ashassi-Sorkabi, N. Gahlebsaz-Jeddi, F. Hashemzadeh and H. Jahani, *Electrochim. Acta,* 51 (2006) 3848.
48. H. Liu, Y.J. Yang, L. Wang, S.M. Ma, X.Y. Peng, D.M. Lu, T. Zhao, Z. Wang, *Int. J. Electrochem. Sci*., 13 (2018) 10718.